

Real-time Grid Reliability Metrics

C.H. Wells¹

Introduction

Electric power grid dynamics have been studied extensively over the past 40 years. Hundreds of technical papers and at least one textbook¹ have been published on this subject, with specific focus on the dynamics of large power systems.

This paper is concerned with the relatively slow dynamics of large interconnected power, both at electromechanical frequencies (~ 1.0 Hz) as well as longer interval dynamic (0.001 Hz) disturbances induced by equipment, market forces, and large power transfers between areas. A set of grid monitoring metrics derived from observations of data just prior to the August 14, 2003 blackout data are outlined in this article. We closely follow the work by Zaborszky² on monitoring the stability of large electric power networks, and we describe work at Entergy on reading phasor measurements (PMU) into a central computer (PDC, phasor data concentrator) to perform real time power system analyses as part of the Eastern Interconnection Phasor Project².

Basis

The discussions on stability³ by Ilic and Zaborszky include the analysis of stable and unstable operating regions and provide numerous examples and specific blackout events, such as Rush Island⁴ on June 12, 1992.

Power systems under stress can violate the “quasi-stationary” (voltage, current, and phase angles change slowly) assumptions used during routine contingency studies. The actual stability boundaries determined using traditional security analysis tools may not represent real conditions; ignoring quasi-stationary has led to erroneous publications⁵

Regardless of the theory used, actual behavior of power systems can be monitored in real time using data from phasor measurement units (PMUs) (absolute phase angles, very accurate measurements of voltage, current, power, flicker, harmonics), at high data rates and time synchronized to GPS clocks. Frequency domain techniques may be used to extract periodic signatures from these time domain data. Observations of these features lead to real time performance metrics. We also show the value of moving window SQC charts, cross-correlation charts, and phase portraits. Each of these real time metrics provide ample advanced warning of a potentially unstable grid condition.

¹ OSISOft, Inc., San Leandro, CA

² EIPP, sponsored by DOE, www.phasors.pnl.gov

We discuss three different sets of datastreams: (1) raw frequency data from New York ISO and the PJM systems just prior to the August 14, 2003, and (2) real time frequency and phase angle data from a substation in southern Louisiana in June 2004, and (3) time synchronized data from Paso Robles, CA and from real time data available at University of Lund³.

Results

Real time data, August 14, 2003

Data used for these analyses were collected from two data archives, one measuring system frequency in the Pennsylvania area, the other in the New York area. The sampling interval varied from 4 to 6 seconds. The data were loaded into a single PI⁴ archive with original time stamps. There is an unknown constant time off-set between these archives. The offset was very small, perhaps less than one second. For the purposes of this study, a time offset is not critical since the analyses are statistical rather than model-based.

The frequency trend chart covering August 14, 2003 is shown in Figure 1. Based on these data,

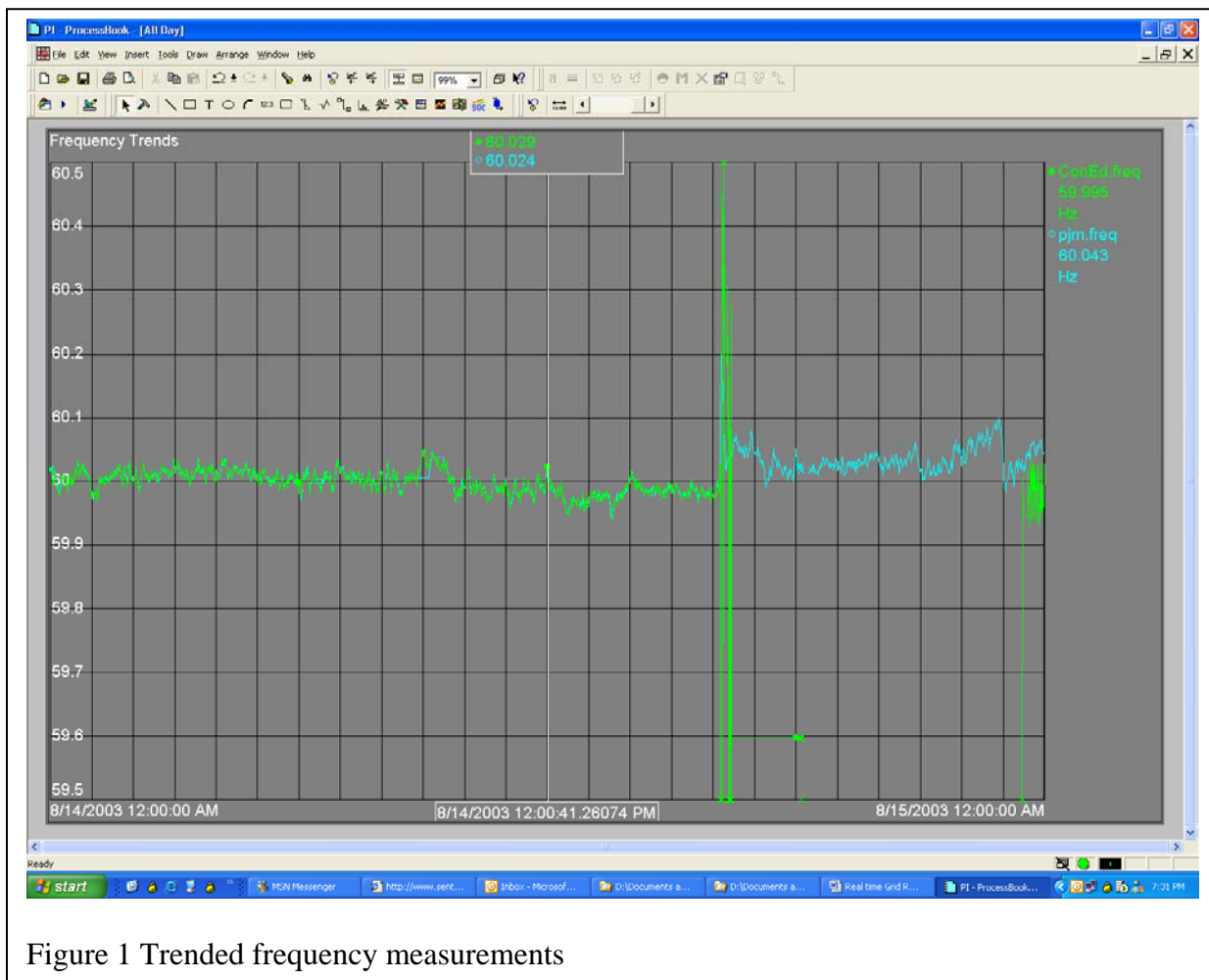


Figure 1 Trended frequency measurements

the collapse occurred at 4:10:52 pm EDT, on August 14, 2003.

The green trend is the frequency measurement from the NY area system; the white pen represents data from the PA area. At noon on the 14th the area frequency setpoint was changed from 60.00 to 59.95.

A detailed view 2.5 hours prior to the blackout is shown in Figure 2.

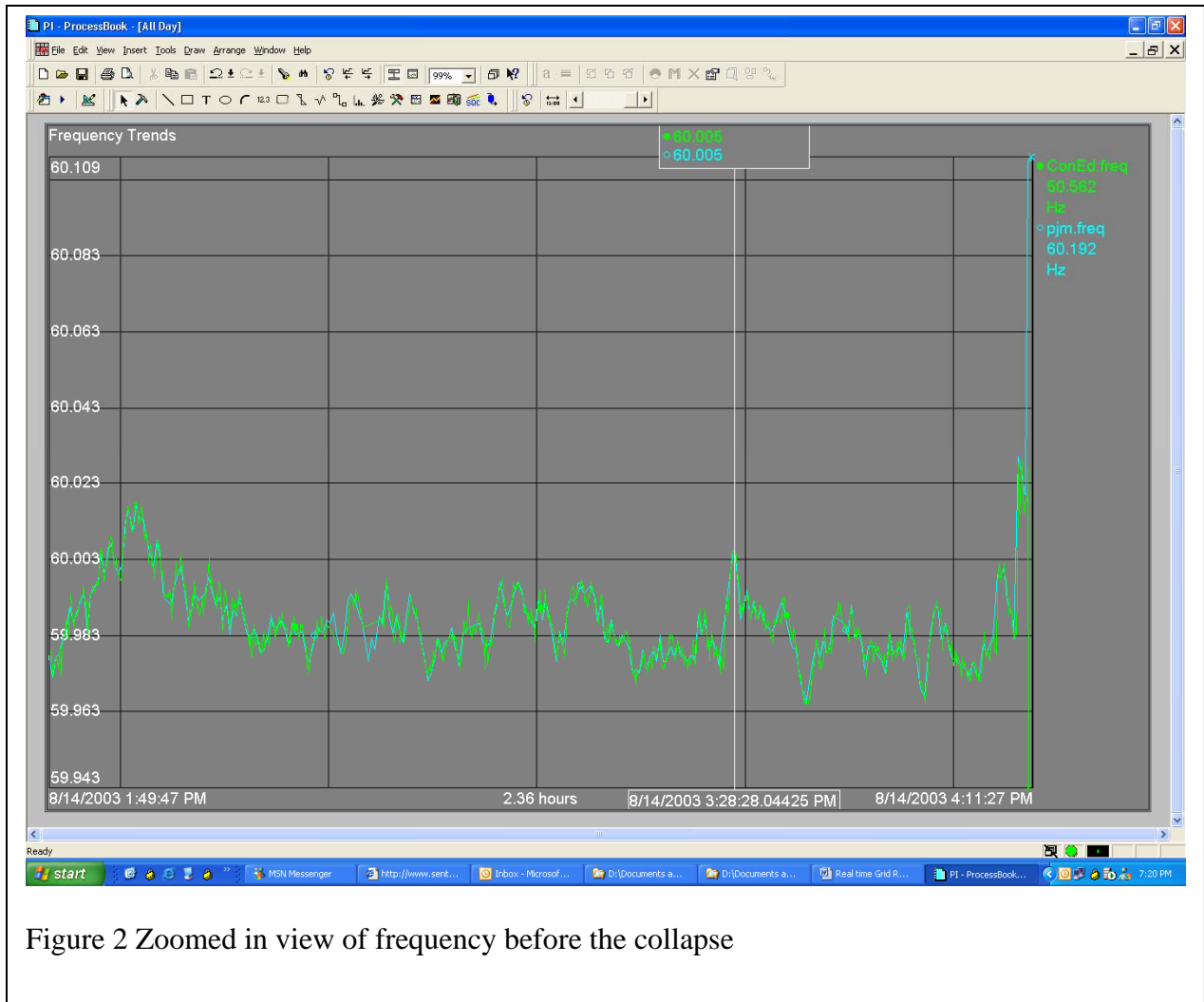


Figure 2 Zoomed in view of frequency before the collapse

This shows that the two frequency measurements were tracking each other closely during the hours preceding the blackout. The data lie directly on top of each other. A more detailed view is shown in Figure 3.

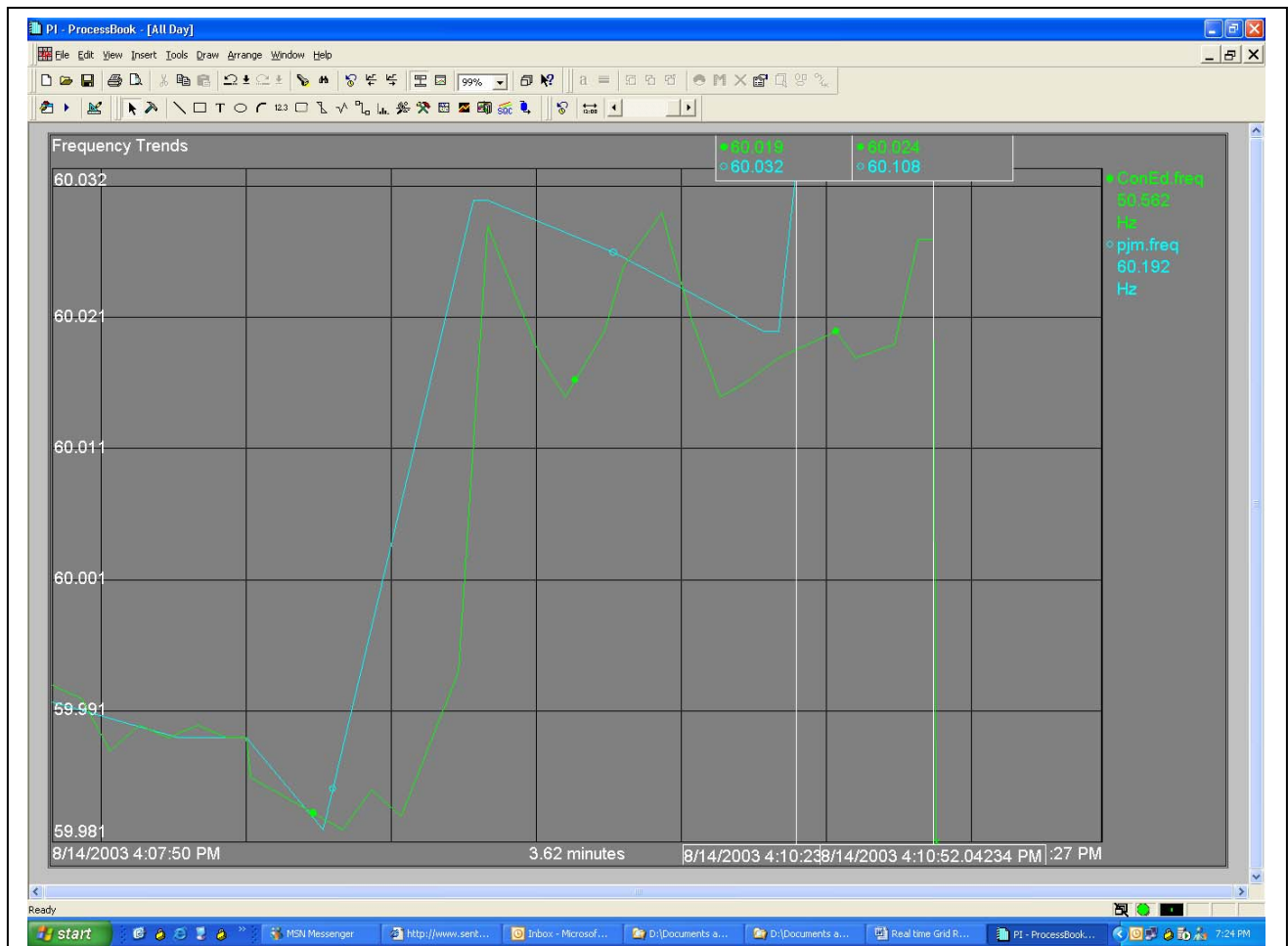


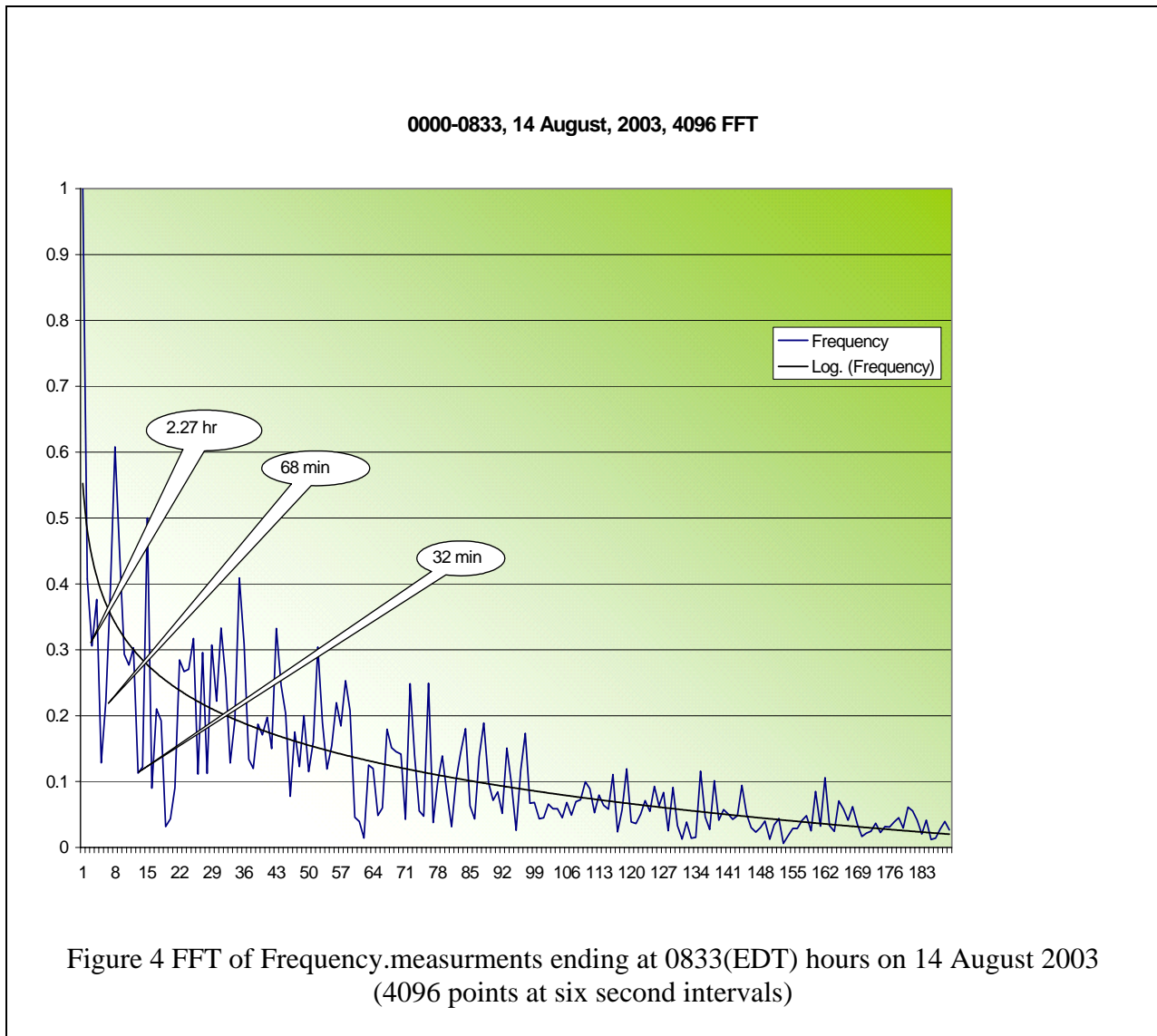
Figure 3. Frequency data just prior to the blackout

This shows the two frequency measurements 3.62 minutes prior to the blackout. The difference between the measurements was 13 mHz at 4:10:23, and 29 seconds later, the difference was 84 mHz. In the preceding part of the day, the differences were much smaller. The differences in measured frequency might indicate a disturbance between the control areas.

Up to the collapse, to the human eye, it appears that the frequency measurements were tracking each other fairly well, as would be expected between frequency measurements within an interconnection. But a detailed view of the data reveals instabilities in the grid.

Real time FFT

Any system considered to be in “statistical control” must have a measured output that can be characterized by a random white noise process. One method of determining this is to compute the moving window FFTs of the process outputs. The shape of the resulting spectrum of a process “in-control” is well known.

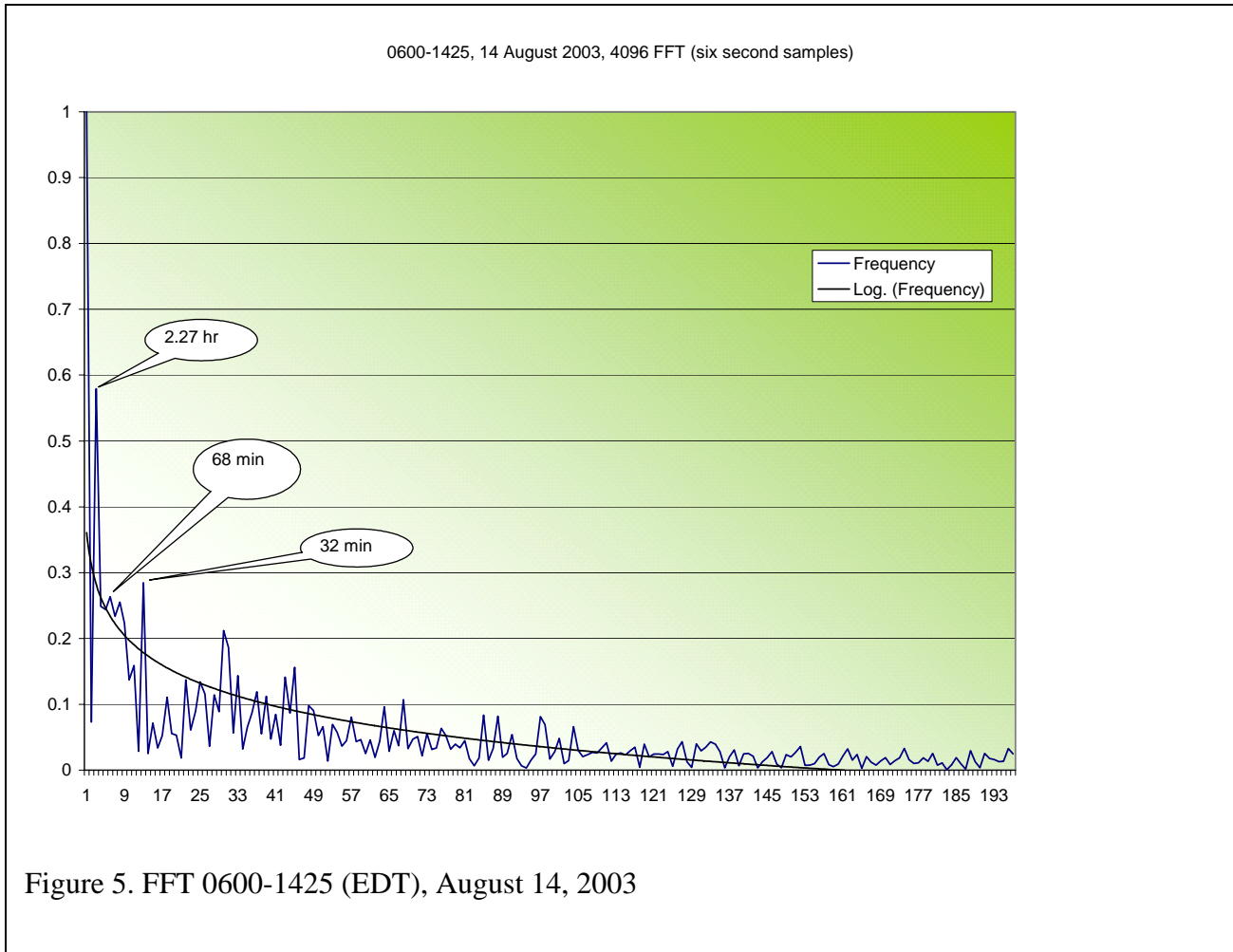


Multiple Fourier analyses of measured frequency collected between the hours of 0000 and 1600 (EDT) on August 14, 2003 were performed as shown in the figures below. Fourier transforms of these data over three time intervals are shown in the following figures.

Figure 4 shows the 4096 point FFT beginning at 0000 hours and ending at 0833 hours (EDT) on August 14, 2003. Notice the relative low power⁵ in the 2.27 hour, 68 minute and 32 minute periods. There are several significant peaks at shorter periods as seen on the right; however, these decay as shown in Figure 5 and Figure 6. At larger harmonic numbers, the traditional electromechanical oscillations can be found.

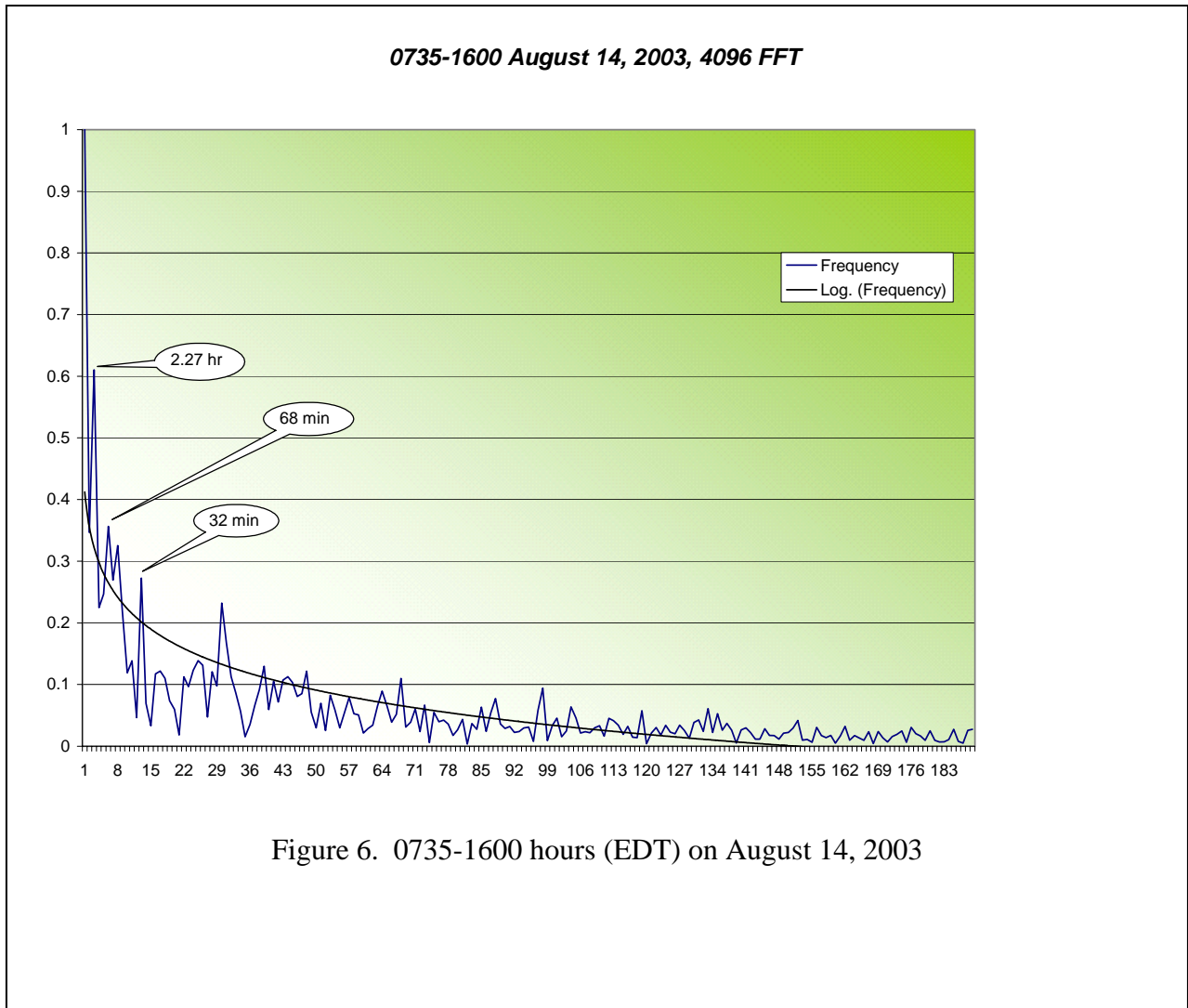
The abscissa is the harmonic number of the FFT; this number can be converted to period in minutes by multiplying the FFT history length times the sample period then dividing by the

⁵ Squaring the absolute value of the FFT gives the Power Spectral Density in each band.



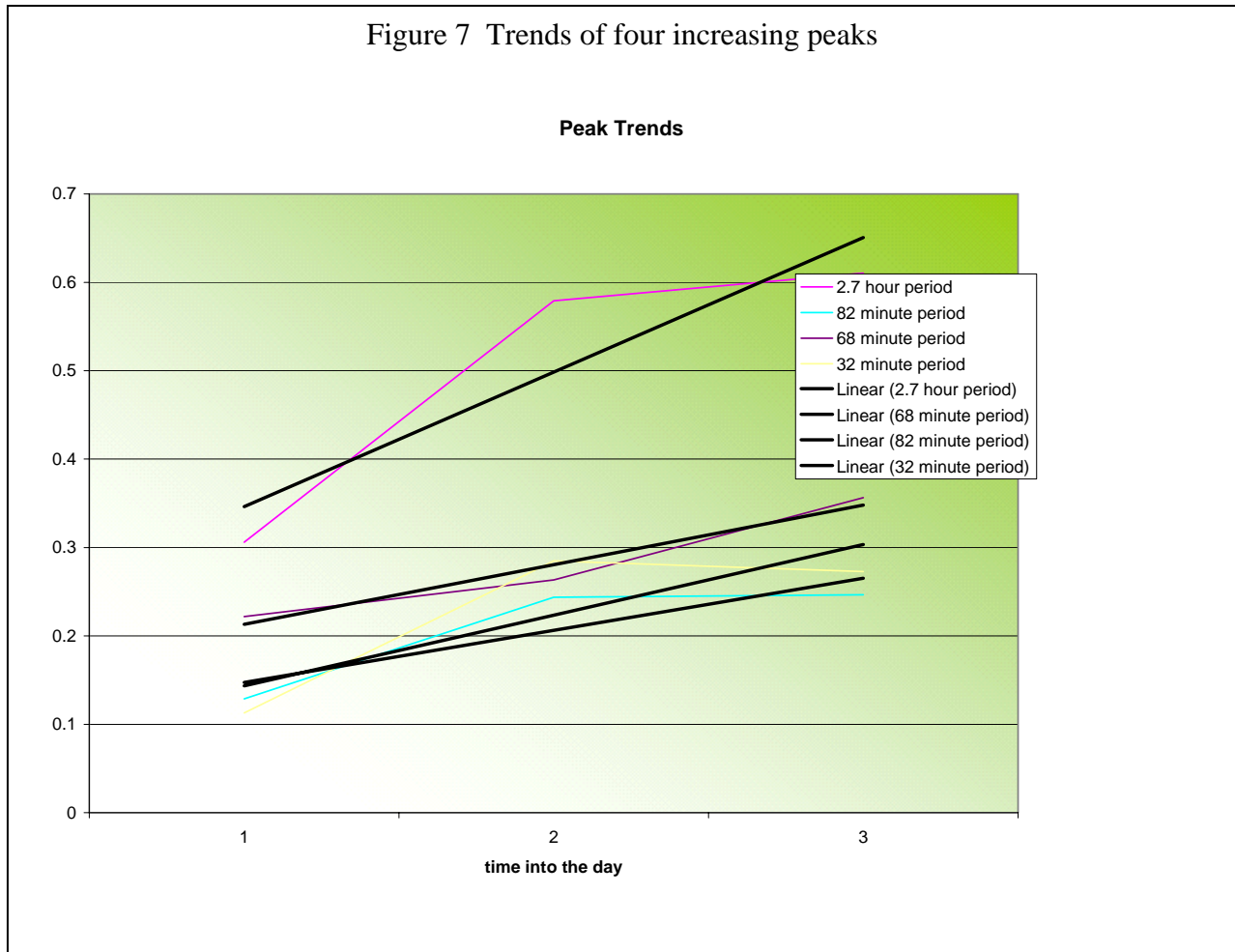
harmonic number. For example, with 4096 samples, six second intervals, the period of the 6th harmonic is: $4096 * 6 / (60 * 6) = 68$ minutes and the period of the 162nd harmonic is 152 seconds.

Six hours later, the amount of power in the noted frequency bands has increased substantially. The power level in the nearby bands as shown in Figure 4 has now dissipated.



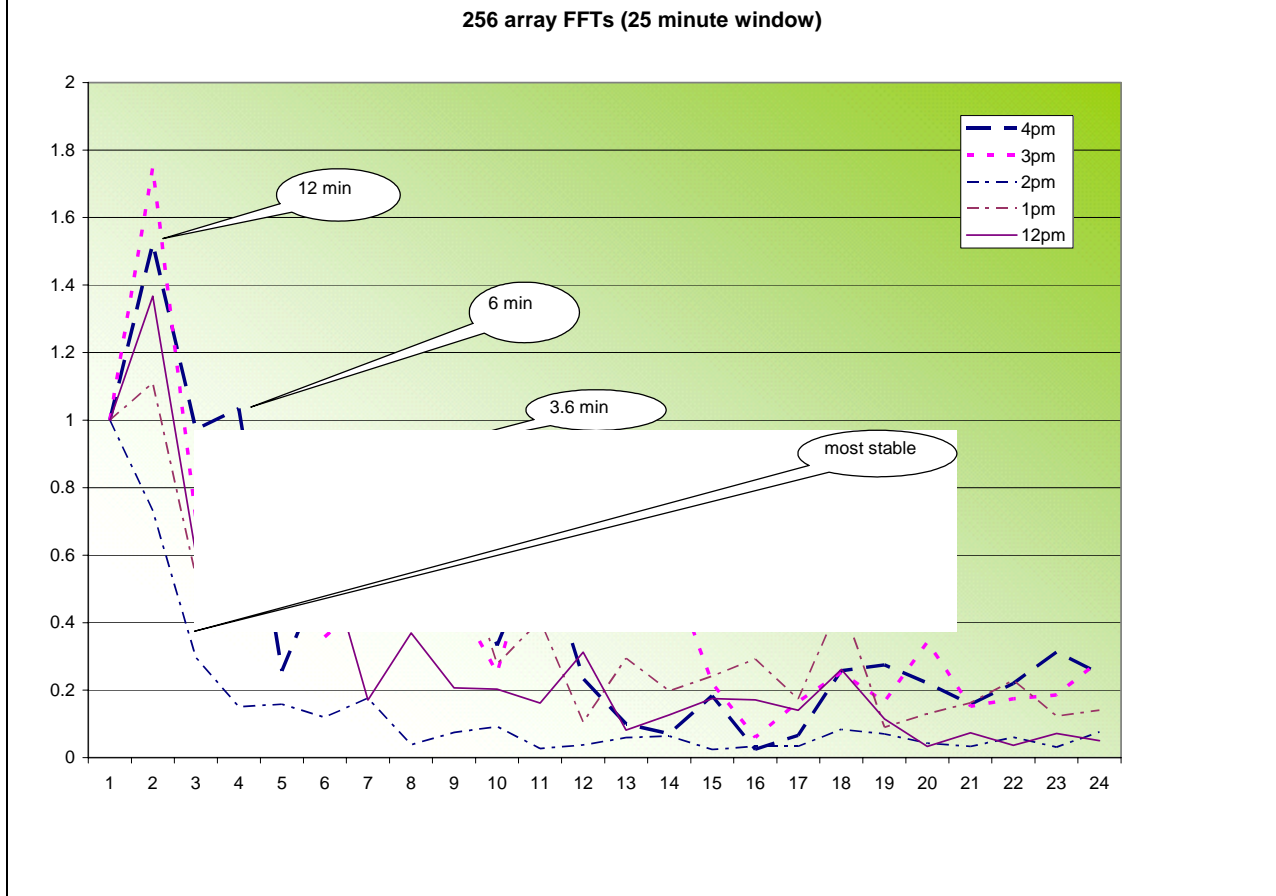
The amplitude of the peaks in the FFT (power) continues to grow in the bands highlighted above. As the day progressed, the power contained in the selected bands continued to increase.

The peak height of selected bands in the FFTs is plotted for each of the three intervals shown above: 1=0000-0833, 2=0600-1425, and 3=0735-1600. These four low frequency peaks grew in amplitude during the day before the occurrence of the blackout.



When using moving window FFTs, the resulting spectra contain periodic information related to the sampling interval and the number of points used to compute the FFT. In the following section, we show the results of running 256 point FFTs ending on the hour, but using the same sampling interval; i.e., six seconds.

Figure 8. Hourly 256 Array FFTs



This shows five FFTs, each computed at the end of the hour using 256 point FFTs. This represents a time interval of about 25 minutes. The conversion from harmonic number to period is given by: $\text{period in minutes} = \frac{256 \cdot 6}{60 \cdot \text{harmonic number}}$. For example, for 7th harmonic, the period is $\frac{256 \cdot 6}{60 \cdot 7} = 3.6$ minutes and the peak at harmonic number 18 represents a disturbance at a period of 85 seconds. The 3.6 minute peak height grew rapidly from 1500 hours to 1600 hours. Interestingly, the spectrum ending at 1400 hours shows behavior we would expect from a stable system; this is the familiar signature of the FFT of nearly random Gaussian white noise.

None of the FFTs have the expected shape of a process under control. Clearly the data are highly correlated as shown by the trend lines. This is clear indication that the spectral shape may be a significant indicator of grid stability.

Figure 9 Hourly 256 point FFTs

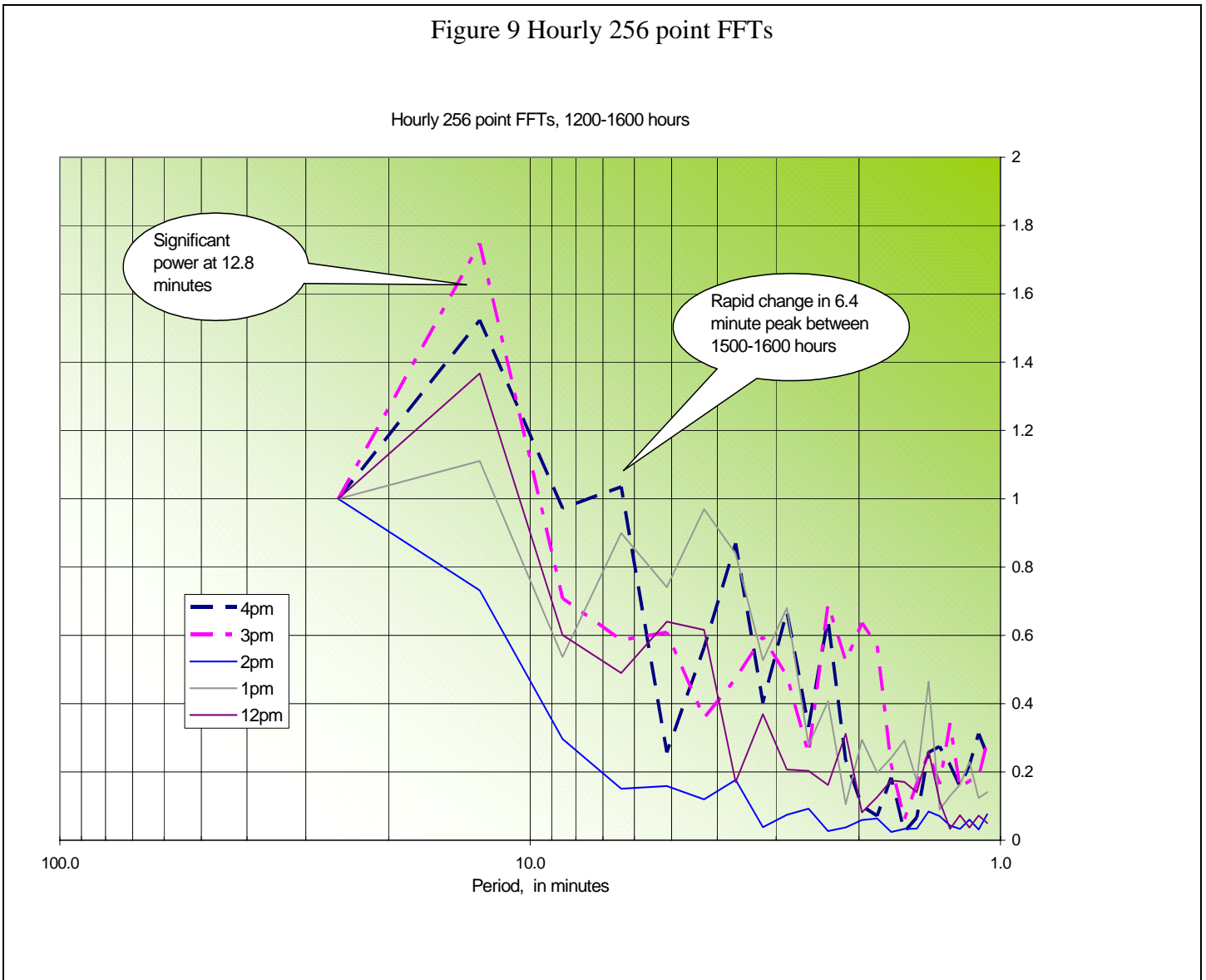


Figure 9 shows the same information as in Figure 8, with the abscissa in log minutes rather than FFT harmonic number.

We also investigated using 2048 point FFTs computed each six seconds during the day. Views of over 9600 of these spectra from midnight until grid collapse are shown in the Appendix.

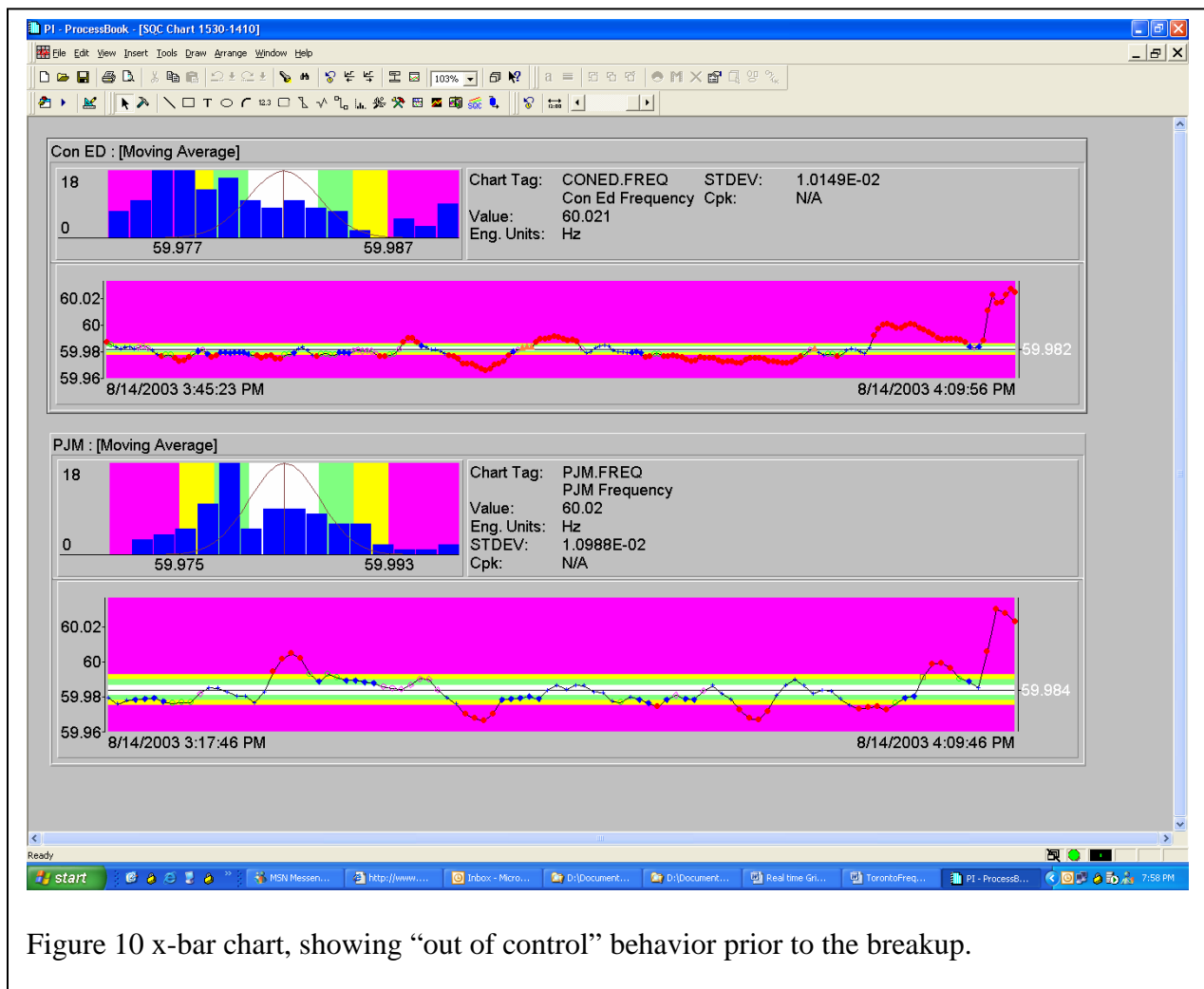
The above analysis clearly shows that there are low frequency oscillations with periods ranging from 85 seconds to nearly three hours in the measured frequency during the 16 hours prior to the voltage collapse on 14 August 2003. If we had data from a PMU at that time, we could

investigate the electromechanical oscillations in the grid at that time, this has been reported by PNL using data from an AEP PMU.

Based on observations that the grid was highly stressed during this period, we believe that moving window FFTs executing in real time may provide advance warning of potential grid instability. Steadily increasing amplitudes in any frequency band are an indication of potential instability. This technology could be used to automatically generate alarms.

Real time SQC

Statistical quality control charts⁶ are used extensively in the process industry. These are mainly applied to the quality variable in continuous manufacturing processes. There are a number of chart types available, typically x-bar, range, sigma and variants of these. The premise behind SQC is any process that is “in-control” will generate an output that is purely random Gaussian



white noise.

Clearly the process is “out of control” for the 10 minutes prior to the blackout. These charts are moving average x-bar charts. Notice also the distribution is not Gaussian also indicating that the

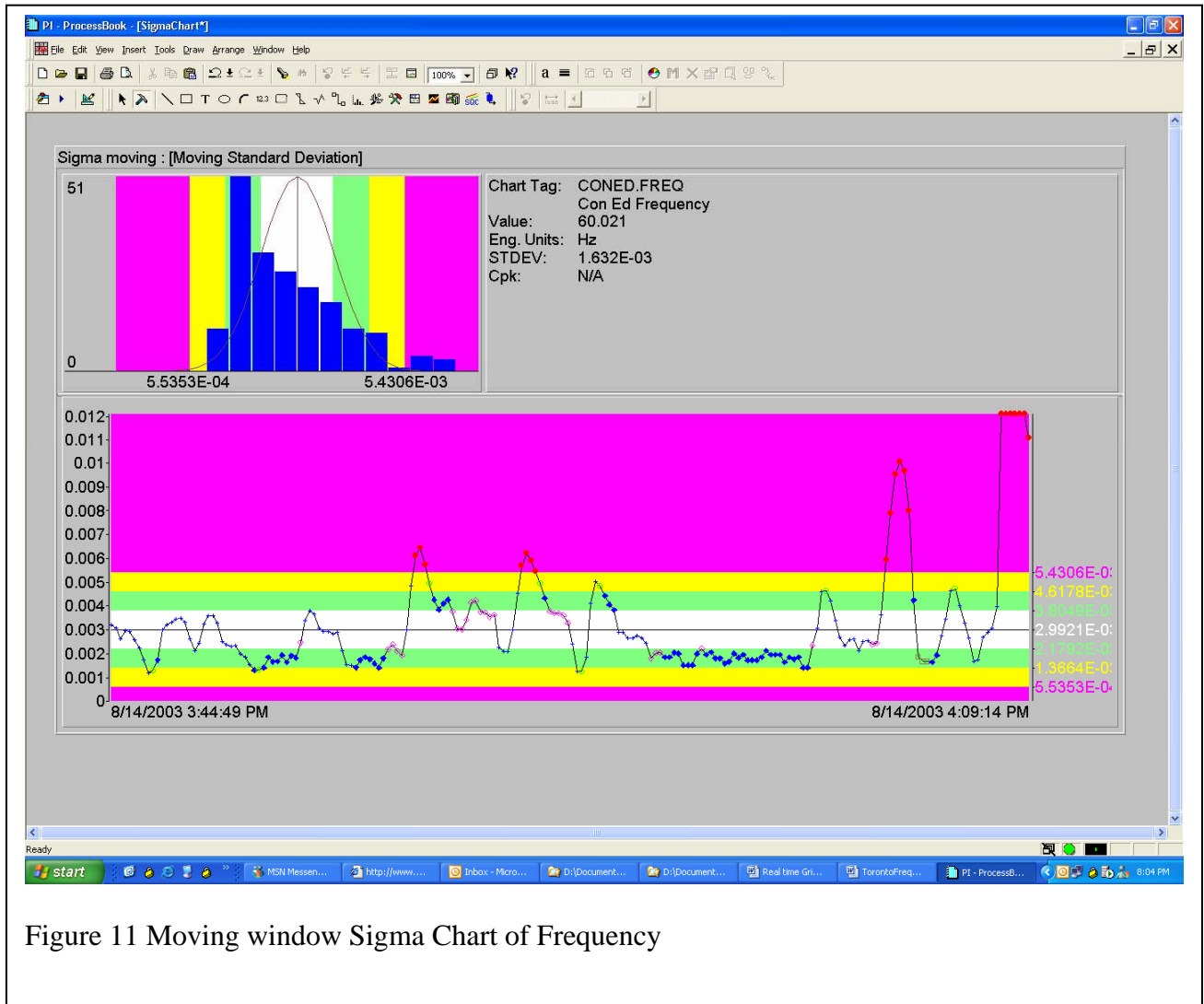


Figure 11 Moving window Sigma Chart of Frequency

“process” is out of control.

This chart also indicates problems before the blackout.

Real time cross correlation

Frequency measurements within an interconnection should be coherent. There will be phase differences accounting for the power flows, but the fundamental frequencies will be nearly identical. The same is true for inter-regional and inter-control area measurements. If we cross-

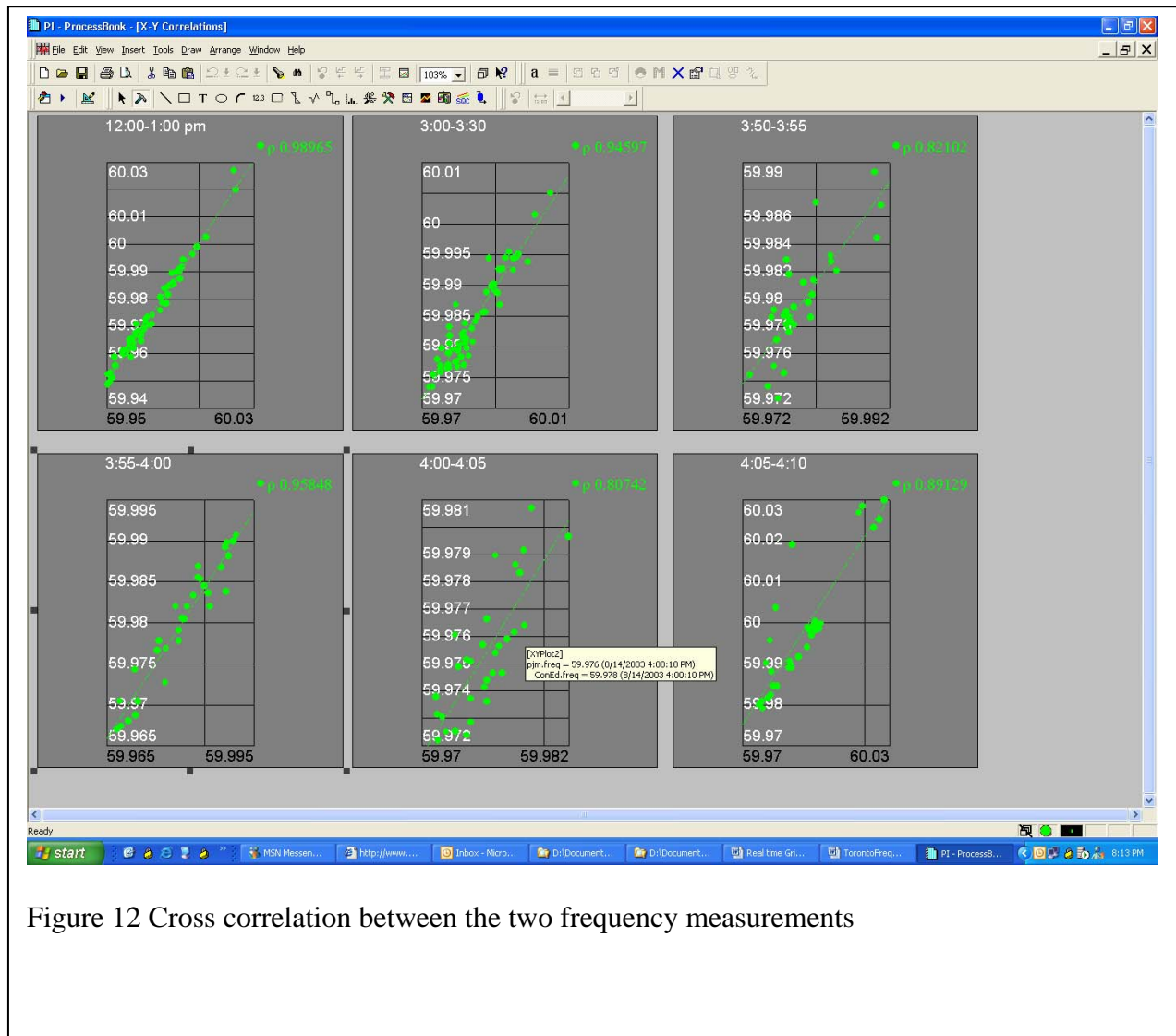


Figure 12 Cross correlation between the two frequency measurements

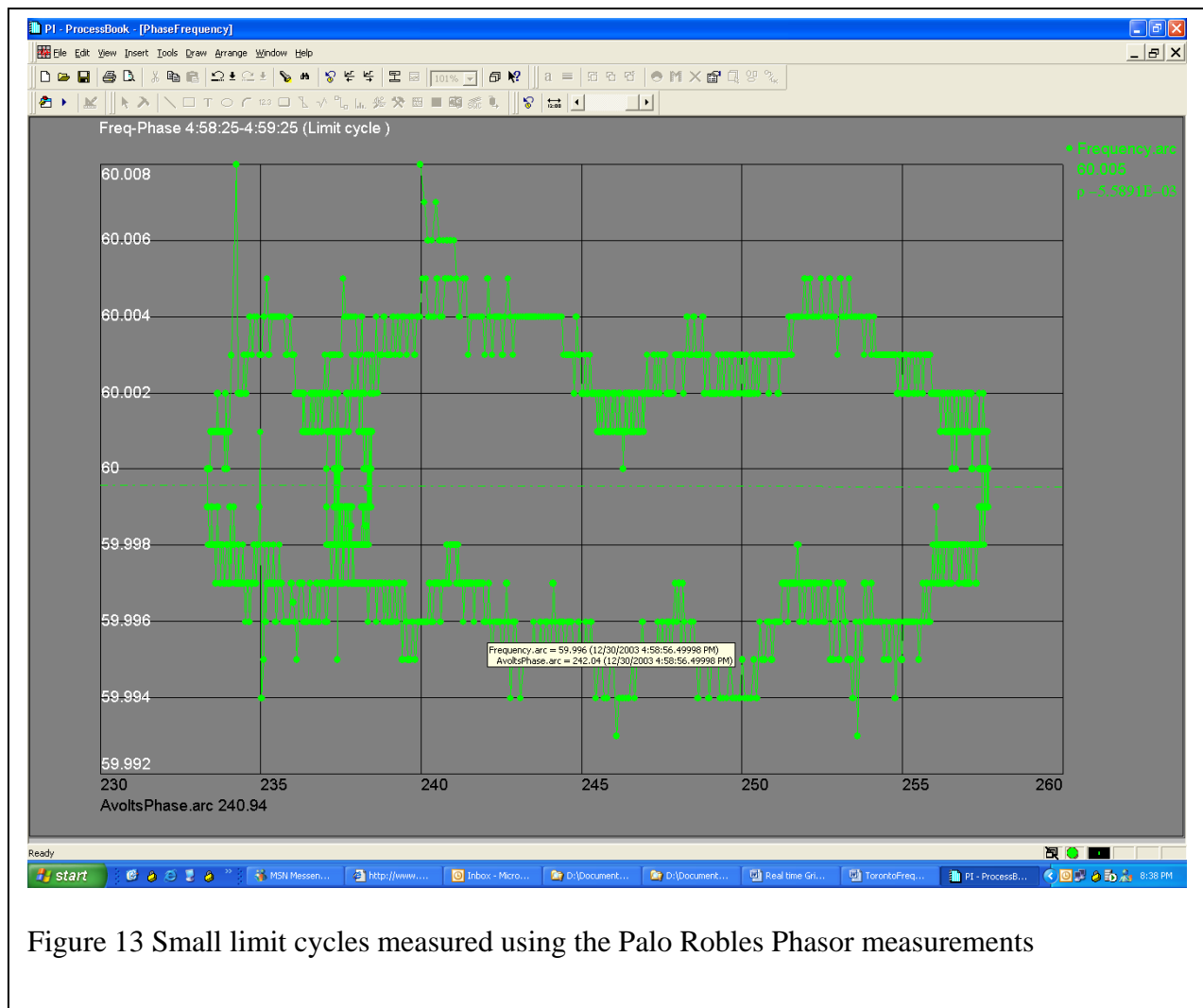
correlate these signals in real time, we observe the behavior shown in Figure 12:

These charts show moving window x-y plots. The correlation coefficient and the linear regression line for the window of interest are also plotted automatically. It can clearly be seen that early in the day there was strong correlation between the frequency measurements as expected, however at the afternoon progresses, the correlation coefficient decreases, indicating

the connection is becoming “less” connected, in other words, the interconnection was losing frequency coherency.

Real time Phase Portraits

Phase portraits are discussed in detail in Ilic and Zaborszky⁷. These plots are implicit time plots of frequency versus phase angle. These are typically used to illustrate limit cycles and unstable equilibria such as Hopf bifurcations⁸. An example of a small limit cycle observed from the Palo Robles phasor measurement system⁹ is shown below in Figure 13.



This is standard x-y plot with a one minute window. Each 1/20 of a second the chart automatically updates, i.e., each plot contains the last 1200 data points.

These charts be configured for wide area phasor measurements and used with bounding boxes to trigger alarms when the limit cycles grow beyond the edges. These charts are often called “snails

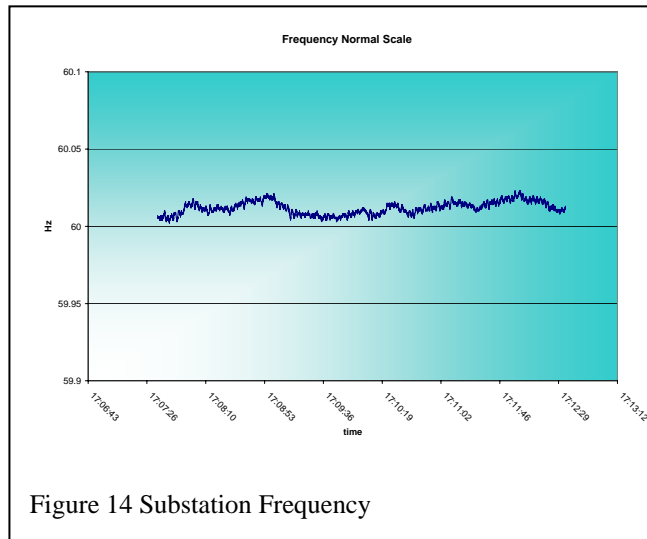
trails” in the Safety Assessment System (SAS) charts required by the Nuclear Regulatory Commission for Nuclear reactor safety.

Entergy EIPP phasor measurement system

Entergy is a member of the Eastern Interconnection Phasor Project (EIPP)⁶ project. Entergy has installed a comprehensive system of ten phasor measurement units distributed across its high voltage transmission grid. The data collected is available to EIPP members in real time via the OPC⁷ interface protocol. The data rates and quality allow us to use these data to estimate grid stability as well as perform a number of other real time control functions.

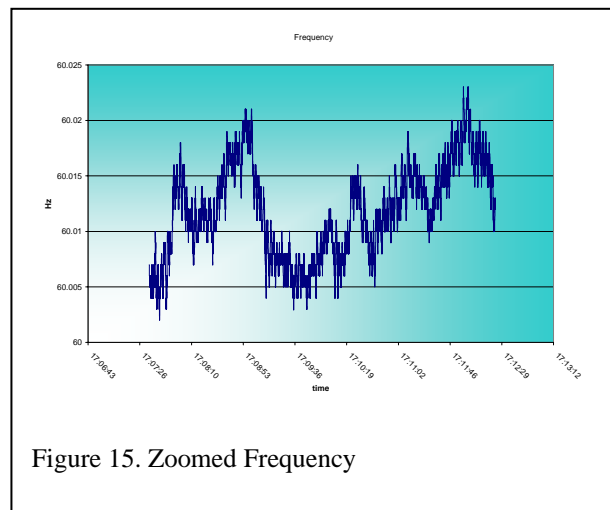
Moving window discrete fast Fourier transforms and their related LaPlace transforms provide a convenient method of determining stability of any type of system and in many respects are equivalent to wavelet analyses, since the time variability component of wavelet analysis is taken into account by the moving window operation.

The electric power grid is a complex system, consisting of thousands of stochastic loads and generators. It is a system that constantly oscillates at characteristic frequencies, typically between 0.3 and 0.7 Hz. These are caused by the both the circuit topology, electro-mechanical coupling between generators, and the characteristics of local loads.



The data shown in Figure 14 is from a 13.5 KV substation on the afternoon of June 9, 2004. The data are collected at the rate of twenty samples per second, each sample with an accuracy better than ± 1 mHz, a substantial improvement over current technology. There are multiple cyclic variations in these data.

The frequency in Hz is shown on the “y” axis and time is shown on the “x” axis. This plot shows 4096 measurements in a typical moving window, about 3.4 minutes in width. Each 50 ms, the trend line shifts to the left, with the newest data appearing on the far right. The frequency scale shown on



⁶http://phasors.pnl.gov/EIPP_News.html

⁷ OLE for Process Control, www.opcfoundation.org

the left is from 59.1 to 60.1 Hz; about the normal for an EMS. This shows small oscillations in the data. With the accuracy available from PMUs, we can extract significantly more information by looking at the fine details contained in the data. This is shown in Figure 15.

In this view, the amplitude scale is 60.0 to 60.025 Hz. Clearly the harmonic content of the data is more evident. One can also observe that the data is intentionally compressed at 0.001 Hz. This is done to reduce the amount of data storage, but does not remove information from the archived data since the accuracy of the measurement device is 0.001 mHz. This is called “lossless compression.” In order to extract the periodic nature of the oscillations in the waveform, we perform real-time fast Fourier Transforms (FFT) on the data.

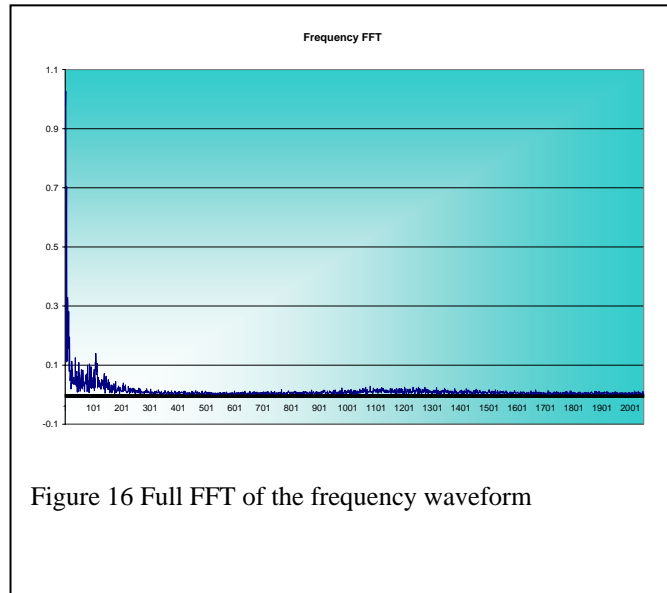


Figure 16 Full FFT of the frequency waveform

A typical “spectrum” is shown in Figure 16. This shows the amplitude of the Fourier Transform computed from a 4096 point moving window. The calculations are repeated every 50 ms on the moving window of 4096 past data points. Only the first 2048 points are shown since the FFT is symmetric about the center point of the array. The normalized value of the spectrum at the first harmonic number is normalized to “one.” This is commonly done to show the details of the spectrum at higher frequencies. The harmonic number increases from left to right. This number

is related to the period of the oscillation by the formula: $\lambda = s * \Delta t / n$, where λ is the period, s is the number of samples in the moving window, n is the “harmonic number,” and Δt is the sampling interval. Any dynamic system “under control” would have a frequency spectrum that shows the characteristics of random white noise: a spike of value 1 at the first harmonic number followed by amplitudes of near zero at higher harmonic numbers. Some use the Akaiki test to determine whiteness of the data. Notice, the frequency measurements are highly correlated and have significant power oscillations at multiple periods. The harmonic numbers are plotted on the x-axis, with the magnitude of the FFT on the y-axis. Note the significant number of peaks in the low frequency range.

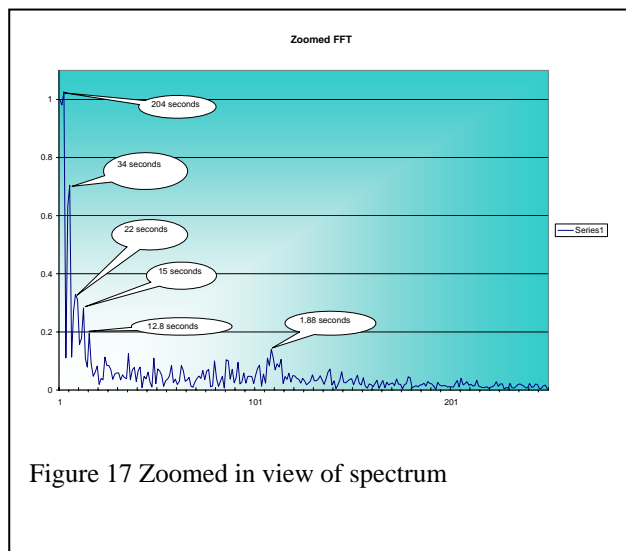


Figure 17 Zoomed in view of spectrum

A zoomed view of this portion of the spectrum is shown in Figure 17.

The five peaks with periods from 204 to 12.8 seconds indicate significant “ringing” in the area around area. These oscillations, if continuing to grow in amplitude, could trip an under or over frequency relay starting a cascading grid collapse.

The grid damping characteristics can be observed directly from these data, by trending the FFT values at each harmonic number. The ratio of successive values of the FFT at each harmonic number is equivalent to the damping coefficient of the grid

The shape of the spectrum also shows how close the grid may be to an unstable operating point. This technology is called bifurcation analysis; and the most common method is called Hopf⁸ bifurcation... The 22, 15, and 12.8 second peaks show the characteristic shapes of bifurcation limits.

The moving window contains 4096 measured values of the harmonics of the waveform. The longest observable period is 204.8 seconds, or 3.4 minutes. The formula for converting from harmonic number to period is $4096 * (\text{sampling interval}) / \text{harmonic number}$. The sampling interval is 0.05 seconds so the numerator is 204.8. To find the period for the 108th harmonic number; $204.8 / 108 = 1.89 \text{ seconds} = 0.53 \text{ Hz}$.

The 108th harmonic number oscillation is close to the 0.7 Hz WECC oscillation. There are a few tie lines across the Northern US and Canada that could communicate this to Louisiana. The spectrum shown in Figure 17 includes six low frequency peaks; there are none above harmonic number 108. The key peaks are located at periods of 204, 34, 22, 15, 12.8, and 1.88 seconds.

PMU’s output absolute phasors: these are not highly useful by themselves. The angle changes at a rate proportional to the distance and direction from 60 Hz. If the angle rate is positive, the frequency is above 60, if negative, the frequency is below 60. But to use angle information for stability, we need at least two meters within a control area. Entergy has a total of ten PMUs feeding data to a central database.

An important point is that the angle calculations have to be done as vectors not scalars. The magnitude and angle have to be converted to real and imaginary components then subtracted as a set. To speed up the phasor calculations we store real and imaginary components, as well as the polar coordinates, so phasor math is easy. We run complex FFTs on these data rather than the real FFTs used on frequency.

Algorithm:

⁸ A summary of this method is shown in the appendix.

The approach suggested is based on classical non-linear stability theory and use of wavelet analyses: a technology that assumes that the wave form spectra are non-stationary. These are described in the literature since the early 80's.

More recent approaches based on clustering coherency methods have also been proposed⁹. The classical non-linear analysis of power systems start with a model defined as

$$\begin{aligned}\dot{x} &= f(x, y, p) \\ 0 &= g(x, y, p)\end{aligned}$$

where x is a vector of the dynamic state variables, y is a vector of the algebraic state variables, and p is a vector of the system parameters. This system is called an algebraically constrained ordinary differential equation describing the dynamics of power system. The eigenvalues of this system can be determined around a linearized operating point. The eigenvalues move in the complex plane (similar to root-locus). As the parameter values change, the location of the eigenvalues (poles) change. The system becomes unstable when any real part of any eigenvalue in the system appears in the right half plane. A bifurcation occurs when the eigenvalues are purely imaginary. This defines a Hopf¹⁰ bifurcation point.

We assume there are N fundamental frequencies in the waveform each represented as a complex eigenvalue. Rather than attempting to solve for the eigenvalues, assuming a valid model existed, we extract the fundamental frequencies then look at their time varying characteristics. Clearly if the damping ratio decreases, the FFT associated with that peak increases implying that the system is becoming unstable.

The time domain approach to determine damping could be used. However, one has to first determine the order of the system, and then run parameter estimation continually on moving data windows. This does not seem to yield useful results since the order of the system changes with changes in grid topology. A recent PhD thesis by M. Hemmingsson¹¹, clearly points this out.

The damping coefficient at each harmonic can be determined by examining the history of the spectrum. If a peak increases in amplitude over time, the grid damping is negative, i.e. the system is going unstable; i.e., the poles of this mode are moving into the right half plane. We suggest computing the peak height derivatives automatically using moving window polynomial filters. This method computes first and second time derivatives in the noisy environment.

⁹ Genc, I, Heinz Schattler and John Zaborszky, "Clustering method in the study of oscillations in the bulk power systems, submitted for publication in IEEE Power Systems, July 15, 2002.

¹⁰ Zaborszky, J., et. al, "Computing the Hopf Bifurcation boundry", EPRI Report, RP3573-10, 1995.

¹¹ Hemmingsson, Morton, Power System Oscillations, Detection, Estimation, and Control, Dept of Industrial Electrical Engineering and Automation, Lund University, Sweden, PhD Thesis (2003) ISBN 91-88934-27-6.

Hopf bifurcations¹² are discussed in detail in Zaborszky's text, Chapter 9. Zaborszky used PEALS, and PSSLF4 to confirm a Hopf Bifurcation caused the Rush Island blackout of 1993 (in this case the topology changed, an insulator at a substation failed). Hopf bifurcations are basically when there are no real parts of the system eigenvalues: this is the bifurcation limit. Any eigenvalue movement to the right will cause the system to collapse.

Hemmingsson¹³ results using phasor measurements taken at low voltage, show striking similarities to work published by the PNNL group. An example of the type of information creates using these data is shown below.

This shows the spectral history of frequency in southern Sweden. Note the increasing energy in several bands, indicating instabilities in the network.

Since, we do not know the actual grid topology at any moment in real time, or the non-linear characteristics of the components in the model, nor do we know the stochastic loads and generation, we believe the best approach to grid stability is to extract this information from accurate phasor measurements. We also demonstrated how to use cross correlations between

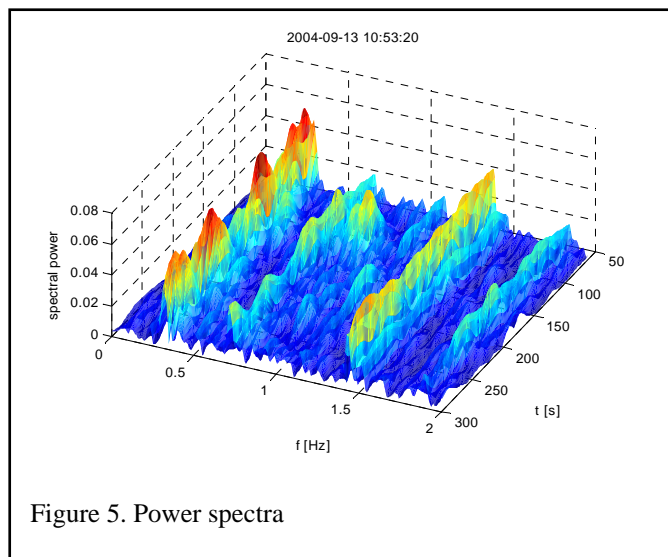


Figure 5. Power spectra

geometrically separate frequency measurements to determine grid coherence. The next level of stability could include computation of the spectral content of relative phasors.

We use moving window polynomial filters to compute the first and second derivatives of the peaks: this is required since the spectra are noisy. The polynomial window width is the "persistence time:" it can be set to any value, for example 5 or 10 minutes, etc. Additionally, since the polynomial coefficients are computed in the filter, we can use these to "predict the future." This is very similar to load

forecasting. We forecast the peaks 5 to 10 minutes in the future. For example, suppose the 108 harmonic peak rate is increasing at 2 times the rate of the adjacent peaks? This indicates potential collapse. The thresholds for limits can be adaptive as well, i.e. they continually ratchet upward. Also for this to work, all other NERC standards must be satisfied; i.e., voltage, current, and frequency have to be within limits.

Calculation of the damping coefficient for each major peak

¹² Abed and Varaiya, in "Int. J. Electric Power Energy Systems, Vol 6, pp 37-43, 1984

¹³ Hemmingsson, M., op.cite, p. 74

Classical second order systems are represented by the equation:

$$\ddot{x} + 2\zeta\omega_0\dot{x} + \omega_0^2x = 0$$

where ζ is the damping coefficient and ω_0 is the undamped natural frequency. If the damping coefficient is greater than one, the system is said to be over-damped, if less than one but greater than zero, the system is under-damped, if equal to zero, the system is oscillatory, and if less than zero, unstable.

However, the grid is more complex than a single second order system with a single natural frequency. Hence we need to compute the damping coefficient for each natural frequency in the system. This can be done using the FFTs as outlined above.

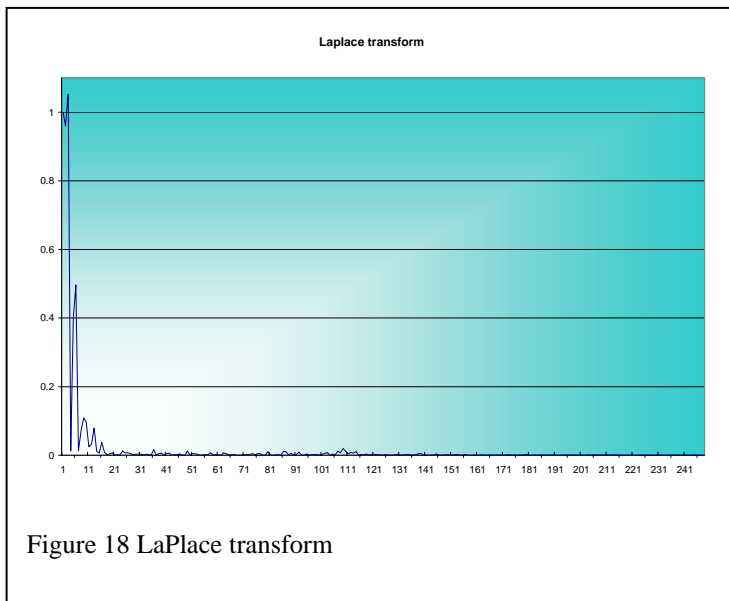
The system uses the history of the spectrum to compute the time derivative of the natural frequencies in the spectrum.

Let $\phi_i(k)$ = the magnitude of the spectrum at harmonic number i at time (k) . Let $\dot{\phi}_i(k)$ be the first derivative with respect to time of this value. Then

If $\dot{\phi}_i(k) < 0$, system is stable

If $\dot{\phi}_i(k) = 0$ system is near instability, a bifurcation

If $\dot{\phi}_i(k) > 0$ system is unstable



These conditions have to be persistent to trigger an alarm. The persistence time is a configurable number, typically far less than the NERC 30 minute persistence limits.

The peak amplitudes vary over time and contain noise. Hence the computation of the time derivatives is done using a moving polynomial filter, typically second order. This produces both the first and the second derivatives and is also used to predict the value of the peak at short periods ahead, typically up to 30 seconds. This is done using the

polynomial coefficients and future time values. We commonly use the linear polynomial as the prediction function, rather than second or higher orders.

The damping coefficient at each fundamental harmonic can also be computed directly from the FFT since the FFT and the Laplace transform are directly related by the square function. So by squaring each element of the FFT, we get the value of the Laplace transform. This is shown in Figure 18.

The damping coefficient is related to location of the poles of the system in units of the Laplace transform as follows¹⁴.

$$\alpha = \frac{IM}{RE} = \frac{\sqrt{(1-\zeta^2)}}{\zeta}$$

where IM and RE are the real and imaginary parts of the poles of a second order system as represented in the S plane.

Or solving for ζ

$$\zeta = \sqrt{\frac{1}{(\alpha^2 + 1)}}$$

Thus, the damping coefficients can be computed in real-time from the moving window LaPlace transforms. This can be done for each harmonic number of significance.

Future Plans:

As part of the EIPP, Entergy offers real time data from (10) ten PMUs. This includes both frequency and phase angle data. Specifically, positive sequence voltage phase angles. These will be located at critical buses in the Entergy network. The PMU data is available to the EIPP using the OPC¹⁵ protocol over a secure VPN connection. The connections are made to an OPC server located in the “DMZ” of the Entergy network. This is a secure area when connections from outside the company can terminate and share data.

Entergy and TVA used OPC to share data in real time. Entergy plans on computing angle differences between the ten phasors for each of the six angle measurements. These will also be used to assess the stability of grid and other network issues.

The phasor differences will be used in the Entergy state estimator to improve its accuracy and validate the assumptions. The positive sequence voltage phase angle and the positive sequence voltages will be used.

¹⁴B. Bequette, Process Control: Modeling, Design and Simulation, Prentice Hall, Dec 2002.

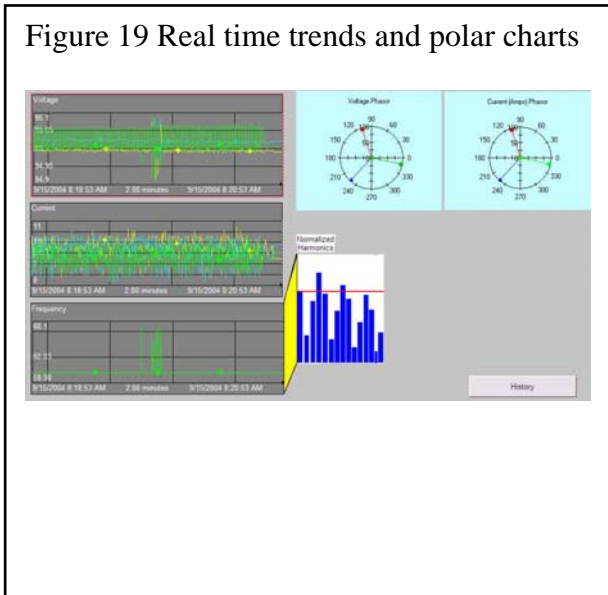
¹⁵ <http://www.opcfoundation.org/>

All data from the ten phasor measurement sensors are stored in a single real time database. This information includes over 110 measurements of power quality for each PMU. The critical information is archived at 20 Hz rates.

Entergy uses a number of features in standard viewing tool to examine the both historical and real time data.

A sample of one display is shown below:

Figure 19 Real time trends and polar charts

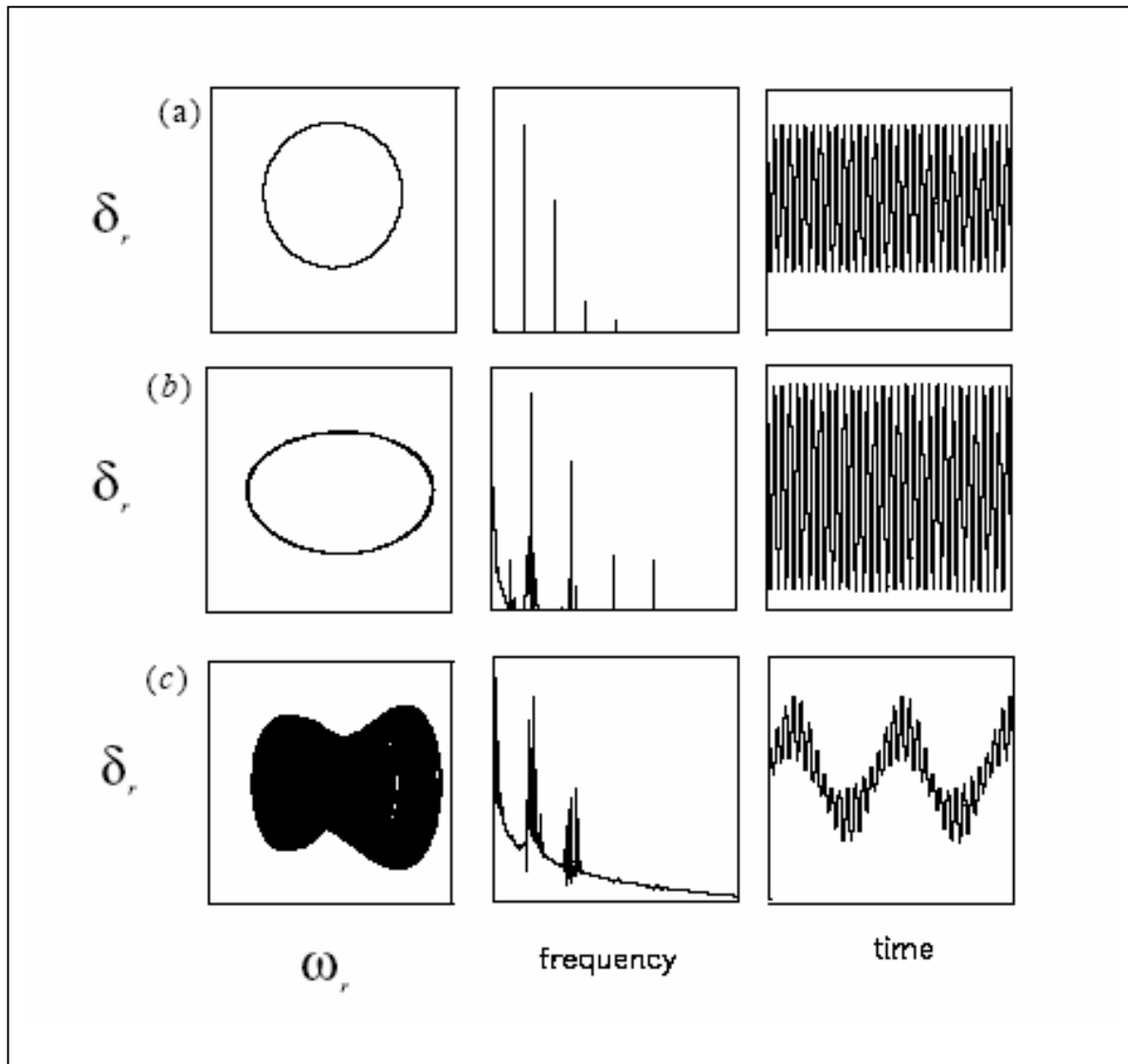


There a number of additional uses of real time PMU data including: state estimation, wide area protection, distance relaying, line sag calculations, real time transfer capacity, and other real time control functions.

Appendix: Hopf Bifurcation

This information was extracted from a recent PhD Thesis published at Virginia Polytechnic Institute¹⁶.

“Figure 3.18: Two-dimensional projections of the phase portrait angle frequency plane(left), the FFT of the corresponding generator rotor angle (middle), and the time traces of the generator rotor angle (right) at $\omega_r =$ (a) 0.5738, (b) 0.59295, and (c) 0.59585. The solution at (a) is a limit



cycle, at (b) is a two-torus attractor recorded well before the blue-sky catastrophe, and at (c) is a

¹⁶ <http://scholar.lib.vt.edu/theses/public/etd-35541228119663620/etd.pdf>

two-torus attractor located just before it disappears in a blue-sky catastrophe.” The shapes shown on the third row of this chart resemble those observed at Entergy.

Conclusions and Recommendations.

We have shown that moving window FFTs, SQC charts, and cross correlation techniques can be used with real time data available in the ISOs and RTOs to help assess the stability of the grid. The resulting analyses can be used by security and reliability coordinators to possibly prevent future blackouts.

Additionally, we believe that real time measurements of frequency and absolute phase angles at strategic locations is an essential step in monitoring reliability of the grid. We also suggest that a common set of real time grid reliability metrics be adopted and used universally by the industry.

Profile Views

This shows more than 10 percent of the total variance of the signal is in the 102-68 minute period. The FFT is scaled to percent of total variance. Times are shown in PDT.

In real time applications, the color map moves upward each time a new FFT is computed, in this case every six seconds.

In grid security applications, we envision the FFTs being computed at least once per second.

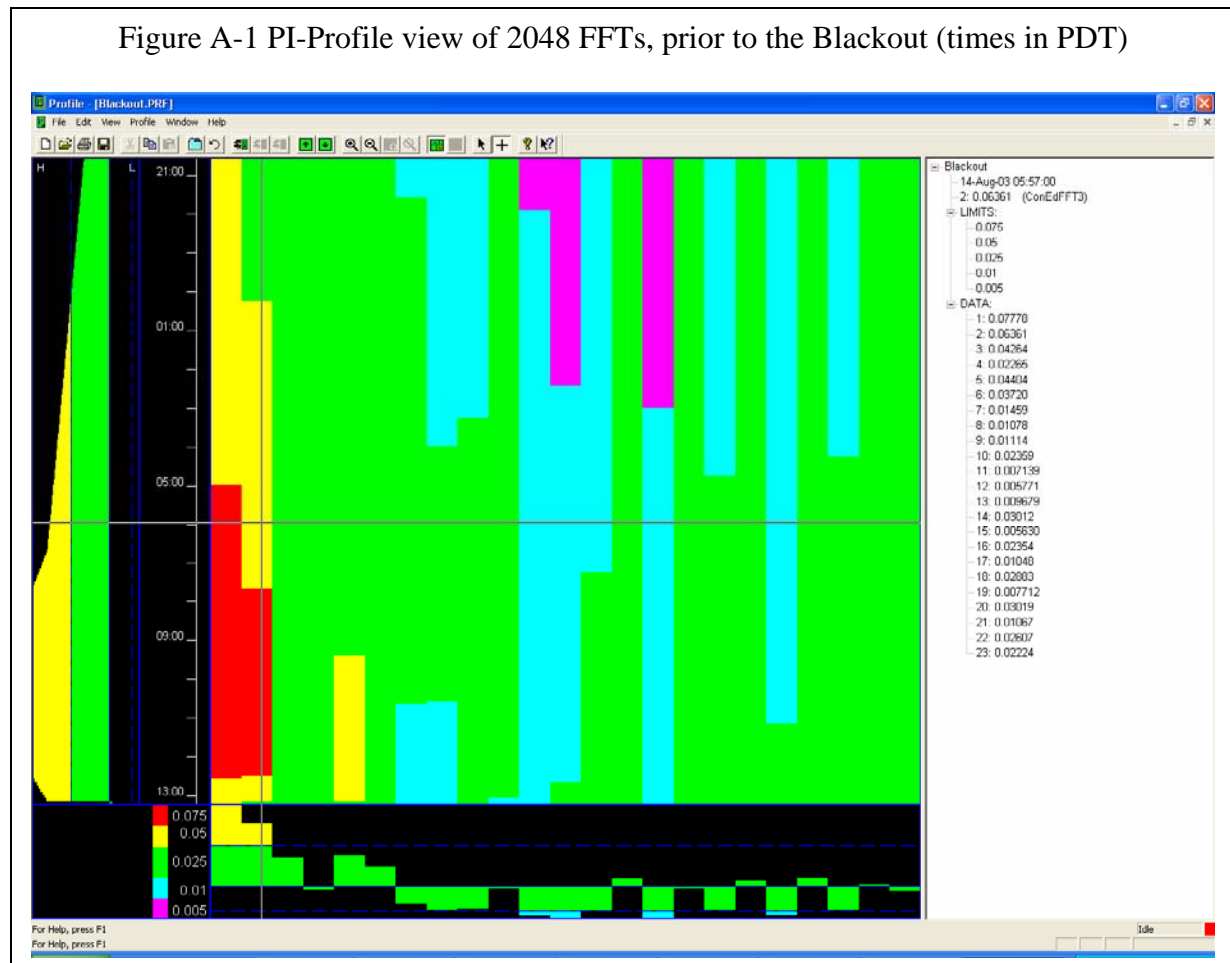
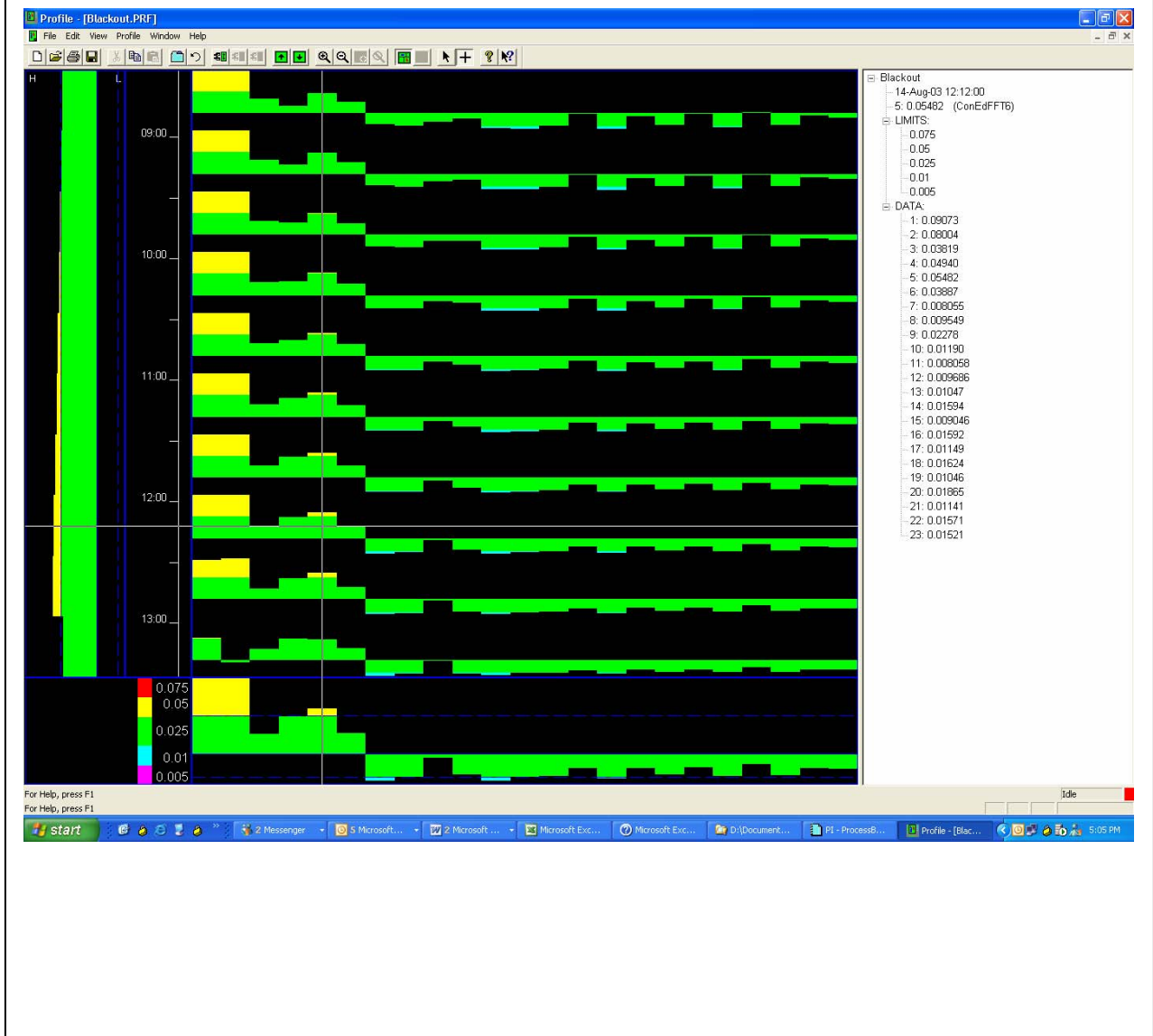


Figure A-2 Waterfall views from PI-Profile (times in PDT)



This shows power growing in the 6th harmonic throughout the day (period = 34 minutes)

References

¹ Ilic, Marija and John Zaborszky, Dynamics of Large Electric Power Systems, John Wiley and Sons, New York, 2000.

² Zaborszky, J, Huang, G., and Zheng, B., New results on stability monitoring on the large electric power systems, Proc IEEE Conf. on Decision and Control, Los Angeles, CA 1987.

³ Ilic, Marija and John Zaborszky, Dynamics of Large Electric Power Systems, John Wiley and Sons, New York, 2000, 391-553.

⁴ Ibid., p 507.

⁵ Ibid., 455.

⁶ Western Electric Co., Inc., Statistical Quality Control Handbook, 2d ed. Easton: Mack Printing Company, 1956.

⁷ Ilic, Marija and John Zaborszky, Dynamics of Large Electric Power Systems, John Wiley and Sons, New York, 2000, p 517.

⁸ Ibid., p 501.

⁹ www.arbitersystems.com